REDESIGN OF AN ELECTRIC MOTOR COOLING FAN FOR REDUCTION OF FAN NOISE AND ABSORBED POWER

J. Vad – Cs. Horváth – M. M. Lohász – D. Jesch – L. Molnár – G. Koscsó – L. Nagy – I. Dániel – A. Gulyás

Department of Fluid Mechanics, Budapest University of Technology and Economics (**BME**)
Bertalan Lajos u. 4 - 6., H-1111 Budapest, Hungary. Email: vad@ara.bme.hu

ABSTRACT

The paper reports on the redesign of an electric motor cooling fan for reducing noise and moderating motor shaft power absorbed by the fan, while retaining the original cooling capacity. The datum fan was a radial flow rotor with radially aligned straight blades. The aerodynamic performance and acoustic behaviour of the datum fan have been measured, in order to establish a basis for redesign. As replacement for the datum fan, an axial flow shrouded rotor with skewed blades has iteratively been designed, involving Computational Fluid Dynamics and Computational Aero-Acoustics. Special flow features, such as reverse flow in the clearance between the rotor and the cover, as well as strong radial flow and deviation due to the motor shield located close downstream, have been taken into consideration in the design. Measurements on the prototype axial rotor confirmed the achievement of the redesign goals.

NOMENCLATURE

c_x	[m]	axial clearance between the shroud inlet plane and the perforated cover
d_t	[m]	blade tip diameter of the radial rotor
Ma	[-]	tip Mach number: u_t per speed of sound in air at 20 °C
N	[-]	blade count
Re	[-]	Reynolds number for the radial rotor: $u_t \cdot d_t$ divided by air kinematic viscosity at 20 °C
u_t	[m/s]	blade tip circumferential velocity of the radial rotor at nominal speed
δ	[-]	diameter factor = $\Phi^{-0.5} \cdot \Psi^{0.25}$ at (nearly) the best efficiency point
ε	[-]	normalized time: time [s] multiplied by rotational frequency [Hz] at nominal speed
η_h	[-]	hydraulic efficiency: ratio between mass-averaged real and isentropic total pressure rise
η_t	[-]	total efficiency: total pressure rise × volume flow rate / input shaft power
η_V	[-]	volumetric efficiency: η_t / η_h
ρ	[kg/m^3]	fluid density
σ	[-]	speed factor = $\Phi^{0.5} \cdot \Psi^{-0.75}$ at (nearly) the best efficiency point
$\Delta\tau$	[-]	normalized temperature change: temperature change × air isobar specific heat × air mass flow rate / motor nominal shaft power, for Φ_n, at 20 °C
Φ	[-]	flow coefficient: for the radial rotor: volume flow rate / ($u_t \cdot d_t^2 \cdot \pi/4$); for the axial rotor: volume flow rate / ($u_t \cdot$annulus area)
Ψ	[-]	total pressure rise coefficient: mass-averaged total pressure rise / ($\rho \cdot u_t^2/2$)
Ψ_S	[-]	suction total pressure coefficient: mass-averaged total pressure upstream of the fan in the measurement pipe / ($\rho \cdot u_t^2/2$)

SUBSCRIPTS

n nominal condition of the radial fan, to be used in redesign

1. INTRODUCTION

Electric motors are often cooled by fan rotors attached to the rear end of motor shaft. Examples for typical rotors and the related flow paths are presented in **Figure 1**. The proportion of dimensions in the sketches does not truly correspond to reality, for better visibility. The air enters the fan via a perforated cover in front of the rotor, directing the cooling airflow towards the cooling ribs located at the motor circumference. Such rotors are frequently equipped with a back-plate, on which the radially aligned straight blades are installed (Fig. 1a). After a quasi-axial inlet, the fluid is diverted radially outward along the back-plate, and is redirected toward the axial direction by the cover. Such radial rotors have the main advantage of having a simple, easy-to-manufacture geometry, and unidirectional operation, i.e. the flow direction does not depend on the direction of rotation. However, the simple blade geometry results in extensive flow separation, increased aerodynamic loss, and pronounced noise. For the possible reduction of fan noise and losses, an alternative is the application of an axial flow rotor (Fig. 1b). In this case, the fluid passes the rotor nearly axially, and is diverted radially outward by the motor shield. If the motor shield is located close downstream of the rotor, a significant radial velocity component already develops inside the rotor.

When designing an axial fan for replacement of an existing radial fan used for motor cooling, a number of aspects, undiscovered in the open literature, are found. Only very few publications report on radial flow rotors with truly radially shaped straight blades, or, in more general, on radial flow blade rows with extremely high incidence. The reports are often confined to the brief presentation of rotor geometry (Noda et al., 2005), occasionally supplemented with a basic aerodynamic survey (Johnson et al., 2007). The studies are confined either to acoustic (Noda et al., 2005) or to fluid mechanical aspects (Johnson et al., 2007), lacking in the combination of the two. To the authors' best knowledge, no information is available in the open literature on characteristic and efficiency curves of radial flow motor cooling fans.

Reports on axial flow automotive cooling fans, operating in a confined environment, provide valuable information for redesign (e.g. Gifford et al., 2006, 2007; Hunt et al., 2009, Moreau et al., 2009). However, it remains a question how the motor shield, located extremely close downstream of the rotor, influences the three-dimensional (**3D**) flow field inside and downstream of the axial flow blade passages, and how such effects are to be considered in blade design. Experiences with automotive cooling fans working under blocked conditions (e.g. Hunt et al., 2009) cannot be utilised directly herein for judgment of interblade and downstream 3D effects. The reason is the absence of the perforated cover in those studies.

The combined aerodynamic and acoustic effects of the radial clearance between the blade tip and the casing have widely been investigated, incorporating various tip geometries, e.g. Corsini et al. (2009). However, no literature source has been found on the aerodynamics and acoustics of axial fan configurations having no "classic" radial clearance – i.e. a shrouded rotor is considered herein – but with an extensive spacing between the rotor shroud and the cylindrical part of the cover, as well as with an axial clearance between the shroud inlet plane and the plane of the inlet perforation.

The present paper gives a summary on an industrial research and development (**R&D**) project, initiated by Grundfos Hungary Manufacturing Ltd. – hereinafter termed as Customer –, aiming at redesigning an existing – datum – radial fan rotor to an axial one, in order to reduce noise emission as well as mechanical power absorbed by the rotor, while retaining the original cooling capacity. During the redesign, the rotor environment – i.e. perforated cover, motor shield, outlet to the cooling ribs – had to be left unchanged.

2. SURVEY ON THE EXISTING RADIAL FAN

The datum radial fan rotor is presented in Fig. 1a. The characteristics of the radial fan are summarized in **Table 1**. The rotor has been subjected to aerodynamic and acoustic experimentation in the built-in configuration, in order to establish a target operational point and quantitative guidelines for redesign. The test rig, capable for characteristic curve and efficiency measurements, is

presented in **Figure 2**. The barometric pressure is measured by means of a digital barometer. A high-pressure fan of variable speed, serving as a booster fan, supplies air to the system. In order to win over the losses in the facility, the application of this booster fan is obligatory for measuring operational states at which the total pressure upstream of the perforated cover is atmospheric – as in the real operational state. The volume flow rate is measured by means of a flow metering pipe with an in-built standardized through-flow orifice meter (ISO 5167, 2003). The differential pressure on the orifice meter is measured by means of a digital manometer, calibrated to an officially certified Betz micromanometer. The air moves from the orifice meter pipe to a measurement pipe, fitting to the diameter of the cooling fan cover, and connected to it in a gastight manner. Preliminary studies revealed that the measurement pipe causes negligible departure from the realistic inlet condition, i.e. free inlet from the surroundings. The temperature in the measurement pipe is measured by a calibrated resistance thermometer. The static pressure upstream of the cooling fan, relative to atmospheric – i.e. in the measurement pipe three pipe diameters upstream of the cooling fan cover –, is measured through four static pressure taps connected to a common piping, by means of a digital manometer also calibrated to the Betz meter. The two-pole asynchronous electric motor operates without shaft load (idle running). The air sucked from the measurement pipe through the perforated cover is exhausted over the cooling ribs. The rotor speed is measured on the shaft by means of a digital stroboscope. The shaft power input to the cooling fan is estimated from the measured rotor speed, in possession of the high-resolution motor characteristic curve (mechanical power output as function of speed) delivered by the Customer. The operational state of the cooling fan is adjusted by the speed of the booster fan. In the real environment, the cooling fan sucks air from the motionless ambient air field, having total pressure being equal to the barometric static pressure. Therefore, the nominal operational state of the fan is imitated in the test facility when the total pressure on the fan suction side in the upstream measurement pipe is just equal to the barometric pressure.

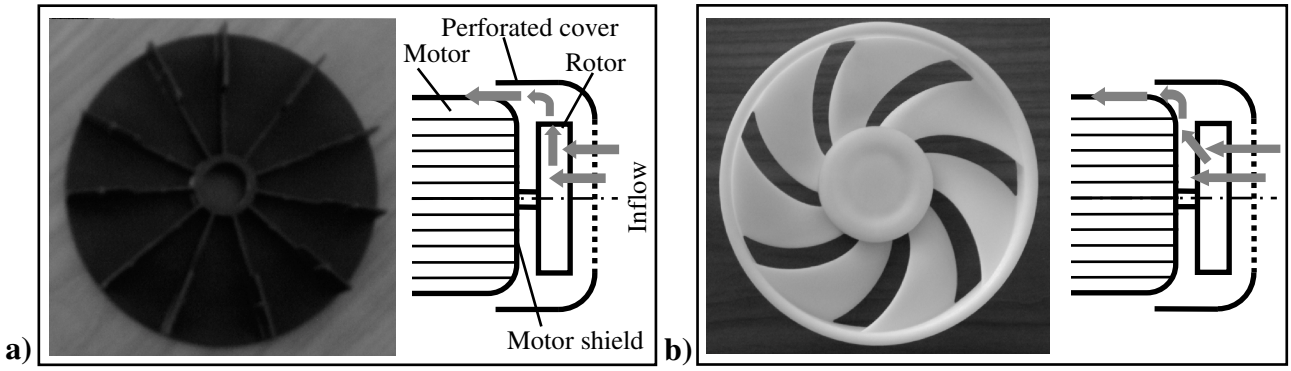

Figure 1. Photo of rotors and simplified meridional scheme of flow paths
a) Radial datum rotor, b) Axial rotor as result of redesign

The experimental uncertainty has been estimated according to the instructions e.g. in ISO 5167, with consideration of propagation of errors, for the vicinity of the nominal operating state used in redesign. Vad et al. (2006, 2007) are given as references for uncertainty estimates. **Table 2** summarizes the *absolute* uncertainty of each measurement-based dimensionless aero-thermodynamic quantity appearing in the paper, valid at a 95 % confidence level. Whenever visible, the uncertainty ranges in Table 2 are indicated in the diagrams using error bars over the entire measurement range.

Figure 3 presents the measured characteristic and efficiency curves of the radial rotor. The nominal operational state has been identified at the flow rate Φ_n at which $\Psi_S(\Phi)$ takes zero value. The corresponding point on the $\Psi(\Phi)$ characteristic curve, i.e. $\Psi_n(\Phi_n)$, specified in Table 1, serves as a basis for redesign. The isentropic total pressure rise has been estimated on the basis of the Euler

equation of turbomachinery, with consideration of slip factor correction judged by Lakshminarayana (1996) to be reasonably accurate for impeller blades having radially aligned trailing edge (**TE**). The hydraulic efficiency η_h has been obtained as the ratio between real and isentropic total pressure rise. Eventually, the volumetric efficiency, η_V, has been calculated as $\eta_V = \eta_t/\eta_h$. As the figure suggests, the estimated η_V data increases nearly linearly with the flow rate. The η_V being relatively low, as compared to usual fan arrangements, reveals that the volumetric loss, representing the reverse flow in the spacing between the rotor and the cover, plays a major aerodynamic role. Therefore, special attention is to be paid to the reverse flow in fan redesign.

Table 1. Radial fan characteristics

N	11
Re	$1.51 \cdot 10^5$
Ma	$5.29 \cdot 10^{-2}$
Φ_n	0.123
Ψ_n	0.322

Table 2. Experimental uncertainty

Φ	$\pm$ 0.001
Ψ	$\pm$ 0.003
Ψ_S	$\pm$ 0.003
η_t	$\pm$ 0.015
$\Delta\tau$	$\pm$ 0.003

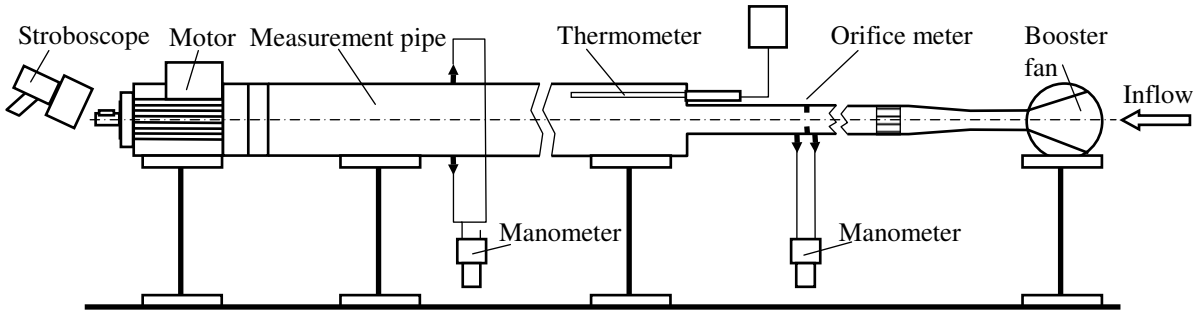

Figure 2. Scheme of facility for characteristic curve and efficiency measurement

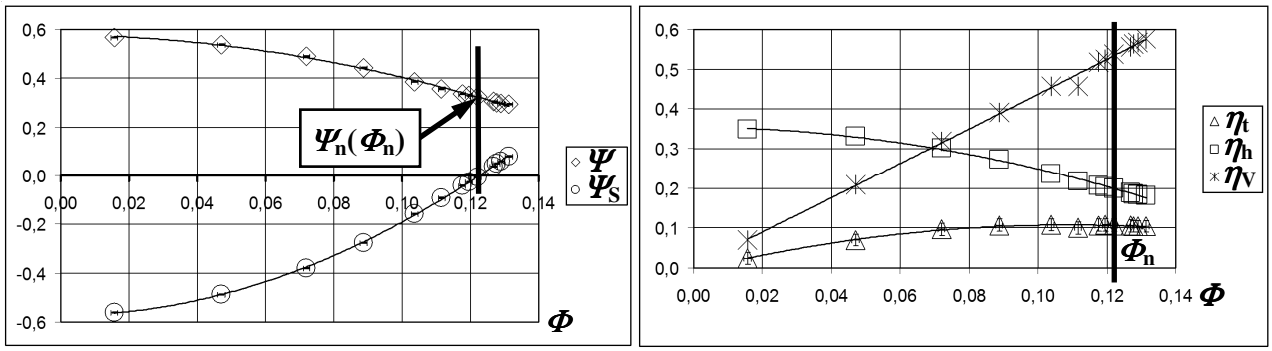

Figure 3. Performance curves of the datum radial fan
Left: characteristic curves, Right: efficiency curves

Acoustical investigations were carried out on the datum radial fan, for the idle running state of the motor, in the reverberation chamber of the Georg von Békésy Acoustic Laboratory. The aim of these studies was to point out the main sources of noise generation. The applied instrumentation was a Brüel&Kjaer 4133 microphone and a Brüel&Kjaer PULSE 3109 type data acquisition system. The measurements were carried out in accordance with the ISO 3743 (1994) standard. The following configurations are discussed herein: 1) motor without fan rotor and without cover, 2) motor with both fan rotor and cover, as shown in the sound pressure level (**SPL**) spectra in **Figure 4**. Only the 0 to 3.2 k*Hz* range is presented for better visibility. The noise of the electromotor is principally generated by mechanical (unbalance, roller bearing, etc.), magnetic (magneto-striction) and

aerodynamic components. The noise signature is indicated in the spectra by tonal components, which peak out of the broadband noise at approximately at 50 and 100 *Hz* and their harmonics. The spectra confirm the dominance of fan noise, underlining the possibilities for noise reduction via redesigning the fan. The fan rotor is characterised by noise generated by its interaction with the steady components, termed herein rotor-stator interaction noise (tonal components within a few times 100 *Hz* broad range), as well as with wake, boundary layer and separation noise (Carolus, 2003) (broadband noise extending to some k*Hz*).

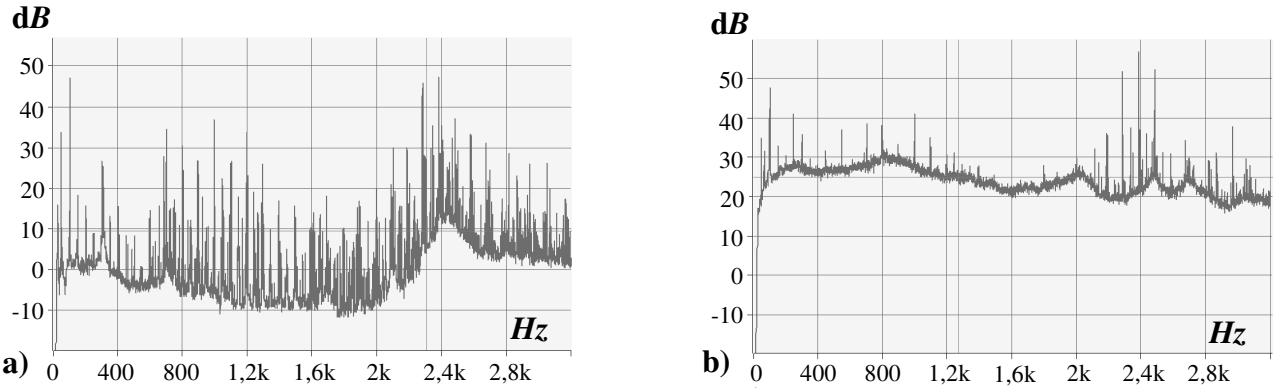

Figure 4. Measured SPL spectra
a) Motor alone, b) Motor with rotor and cover

3. COMPUTER-AIDED AXIAL FAN DESIGN

The following section briefly outlines the methodology and the guidelines applied to combined, iteratively applied aerodynamic design and „sound design" (Carolus, 2003) of the axial flow fan by which the datum radial fan is to be replaced. The iterative modifications resulted in the final axial fan geometry presented in Fig. 1b. As instructed by the Customer, the geometrical, measurement and computational details of the axial rotor are disclosed herein in a limited manner only, for confidentiality reasons.

In fan redesign, based on the $[\Phi_n, \Psi_n]$ data, the axial rotor blade tip diameter has been modified, and therefore, the flow and total pressure rise coefficients have been re-calculated for the new axial rotor. On the basis of these modified coefficients, the data couple of diameter and speed factors $[\delta,\sigma]$, have been calculated and presented in the Cordier diagram (Carolus, 2003) for the new axial fan, as shown in **Figure 5**. The diagram suggests that the design target could be realized by means of a mixed flow fan – higher flow turning capability – rather than by means of an axial rotor. Still, an axial rotor was selected for the final configuration, according to the instructions of the Customer, given that it can be mass-produced by means of a more simple injection moulding device. The demand for relatively high flow turning forecasts the challenge of designing an axial flow fan of unusually high blade load.

The design process has been aided by Computational Fluid Dynamics (**CFD**) as well as by Computational Aero-Acoustics (**CAA**) means. Steady flow simulations were carried out by means of the commercially available finite-volume CFD code Fluent (2006). Preliminary to axial rotor modelling, validation studies were carried out on the basis of the radial rotor. The k-ω SST model was found to provide the best fit to the experimental data, and therefore, it has been used in the axial rotor CFD as well. The final choice of this turbulence model is also in accordance with the guidelines given by Kelecy (2010). Sensitivity studies were carried out on setting the extension of the blow-out zones to various sizes. In the final CFD model, independence from the blow-out zone size has been achieved. At the sides of the blow-out zone, the boundary condition was "pressure-outlet". **Figure 6** presents the computational domain for the axial rotor in an intermediate design phase. Taking periodicity into consideration, the computations regarded only one blade pitch.

Utilizing the features of the annular cascade configuration, boundary conditions of periodicity were applied. The inlet face is a sector of the circular measurement pipe with 360°/7 central angle (7 blades were considered). Downstream of the inlet face, sectors of the pipe and the rotating hub with one blade in the middle of the domain are included. At the inlet face, a swirl-free steady inlet velocity profile belonging to a fully developed flow is given corresponding to the actual flow rate. The reasonability of fully developed flow assumption has been verified on the basis of preliminary CFD studies on the measurement pipe. The inlet turbulence intensity has been set to 1 %, and the hydraulic diameter was set to the diameter of the pipe. A structured hexahedral mesh has been developed for the entire computational domain. About 50 % of the cells are located in the refined domain in the vicinity of the blade. The rotor geometry is relatively complicated, and therefore, the fan zone is separated into a number of blocks. Around both the blade and the shroud and near the walls of the motor and the fan cover, O-type mesh is applied, while an H-type topology is applied for the rest of the rotor blade passage. 95 % of the cells have an equiangle skewness of less than 0.75. The highest skewness values appear near the common edge of the shroud and the blade, due to the complicated topology. The majority of y^+ values fell within the range fulfilling the requirements of the applied low-Reynolds number wall law. Typical computations required approximately 3-4000 iterations. The solutions were considered converged when the scaled residuals of all equations were resolved to the levels of order of magnitude of 10^{-3} and the surface monitors remained practically constant.

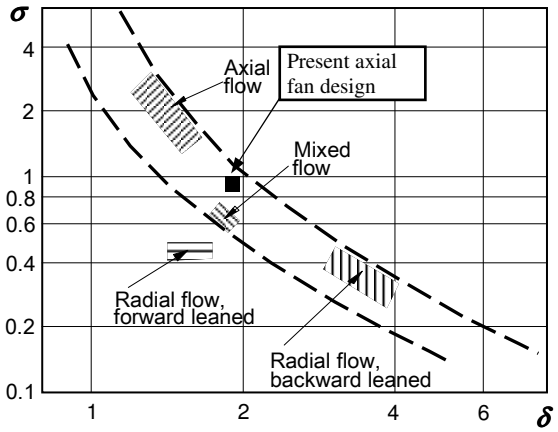

Figure 5. Cordier diagram for optimum [δ,σ] data couples

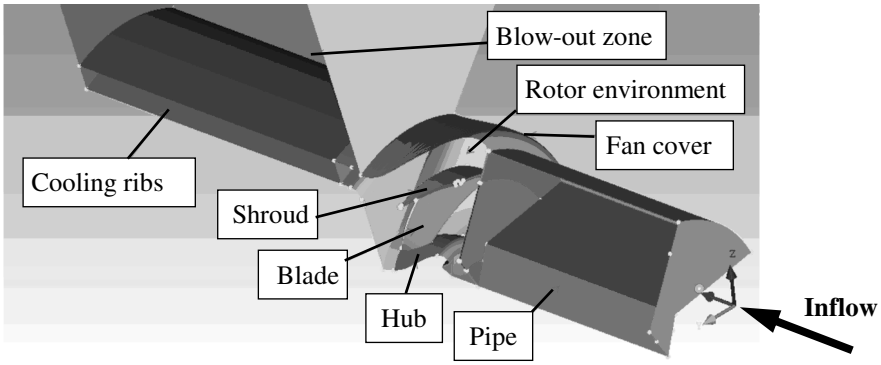

Figure 6. Computational domain for the axial rotor

The applied CAA technique, based on the CFD results for obtaining qualitative acoustic information, is reported in Horváth and Vad (2009). The steady CFD simulations served as basis for CAA survey on broadband noise sources. The acoustic source terms have been estimated on the walls on the basis of boundary layer parameters, as well as in the free shear layers. The use of this methodology has been inspired e.g. by Cros and Carbonneau (2009).

In what follows, the main features of aerodynamic and acoustic design are outlined.

Aerodynamic design aspects

The controlled vortex design (**CVD**) technique (Vad et al., 2007), prescribing spanwise increasing blade circulation along the dominant part of blade height, has been applied. The benefits of the CVD method in the present design assignment are as follows. 1) The blade sections at higher radii are better utilized, generating locally higher axial velocities. This fits to the circumstance that the cooling fan should perform dominantly at outer radii, near the location of the cooling ribs. 2) The increased performance contribution of blade sections at higher radii also matches the demand of high specific performance (see the Cordier diagram). 3) In order to moderate fan noise, the rotor circumferential speed is to be limited (e.g. Carolus, 2003). At a prescribed performance, this can be carried out only by means of CVD, i.e. by better utilization of blade sections at higher radii. 4) Near the hub, the stall and aerodynamic blockage are expected to be pronounced, due to the presence of the hub and the motor shield (Gifford et al., 2006, 2007). By means of CVD, the hub diameter can be purposefully reduced, and near-hub blade sections can be unloaded, leading to the moderation of near-hub loss.

In the preliminary design phase, the air velocity data has been correlated with linear cascade measurements on the basis of Wallis (1983). Blade sections of circular arc camber line and of uniform thickness, with a rounded leading edge (**LE**) and TE, have been applied. This simple geometry is beneficial from manufacturing point of view. Furthermore, at the low chord-based Reynolds number, valid for the present case, such blade sections show better aerodynamic performance than profiled blade sections (Carolus, 2003).

Strong reverse flow has been experienced from the downstream to the upstream region of the axial rotor, over the shroud and in the axial clearance between the perforated cover and the inlet region of the rotor shroud. As an example, section b) in **Figure 7** shows a meridional section of the axial rotor and its environment in an intermediate design phase. In Fig. 7, the white zones correspond to cuts of the shroud. The leakage flow interacts with the incoming main flow, resulting in a pronounced vortical phenomenon near the shroud, and influencing the flow conditions along the entire span in an unfavourable manner. Section c) of the figure demonstrates that, when the axial clearance was virtually reduced to zero in the CFD simulation (by a surface indicated approximately by a bold line segment), the leakage flow and the related unfavourable effects have been eliminated. Section b) in **Figure 8** demonstrates that an extensive separation zone develops near the LE on the pressure side, due to high negative incidence, due to the effect of leakage flow generating local inlet axial velocity higher than design. A virtual elimination of axial clearance – Fig. 8 c) – remedies the unfavourable incidence condition; the separation zone disappears. During the design process, the direction of the blade LE has been adjusted for achievement of favourable incidence, for moderation of near-LE separation even in the presence of leakage flow.

Experiments were carried out to survey how the axial clearance size influences the volumetric losses, and thus, the volume flow rate delivered toward the cooling ribs. **Figure 9** presents the experimental data on the flow rate as a function of axial clearance size. The flow rate has been found to fall nearly linearly with clearance size.

In the preliminary design state, the effect of downstream blockage, caused by the vicinity of the motor shield, has approximately been considered on the basis of (Gifford et al., 2006, 2007; Hunt et al., 2009). Compared to flow deviation correlations valid for linear cascades (e.g. Lieblein, 1965), significantly increased flow deviation from the blade TE direction was experienced, caused by the vicinity of the downstream blockage (motor shield). It has been compensated, by increasing the flow turning capability of the blading. As suggested by Figs. 7 to 8, the interblade flow is characterised by radial velocity reaching the order of magnitude of that of axial velocity. Accordingly, the blade sections were designed by modelling conical stream tubes through the rotor.

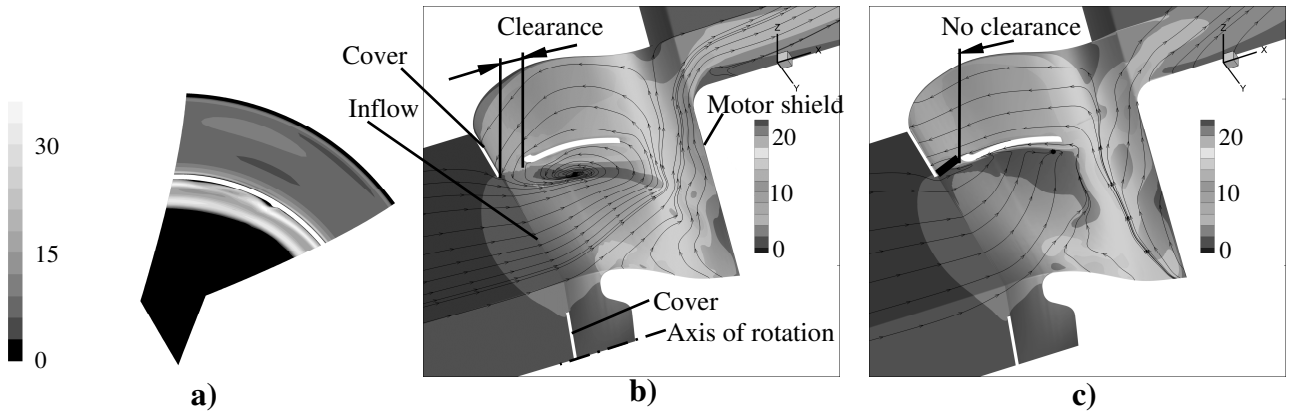

Figure 7. CAA and CFD results. a): c_x = 5.2 % d_t. Acoustic power level [d*B*] at the plane normal to the rotor axis just downstream of shroud inlet. b), c): Streamlines and velocity magnitude [*m/s*] in a meridional section. b): c_x = 5.2 % d_t. c): No clearance.

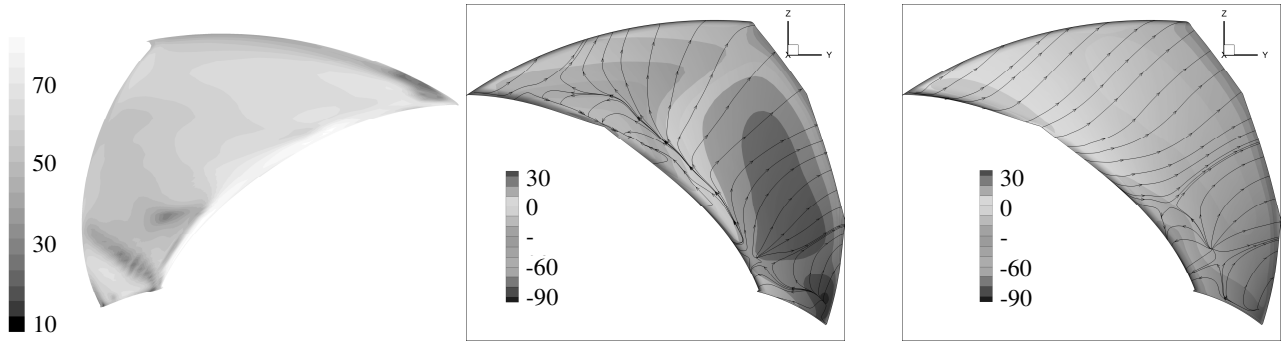

Figure 8. CAA and CFD results related to the blade surface. a): c_x = 5.2 % d_t. Acoustic power level [d*B*] on the suction side. b), c): Limiting streamlines and static pressure [*Pa*, relative to atmospheric] on the pressure side. b): c_x = 5.2 % d_t. c): No clearance.

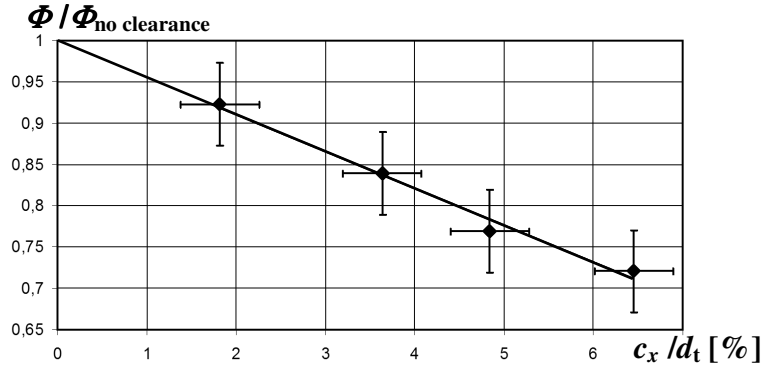

Figure 9. Dependence of flow rate on axial clearance size: measurements

Acoustic design aspects

It has been considered that if the blade tip Mach number is below approximately 0.1, an axial fan without guide vanes can be expected to be less noisy than a radial fan (Carolus, 2003). Circumferential forward skew ("sickle-shaped" blades) has been applied for the reduction of rotor-stator interaction noise, and for the reduction of boundary layer noise (due to thinner boundary layer

on the suction side of the highly-loaded blades), as well as for achieving aerodynamic improvement (Carolus, 2003).

The CAA data in **Fig. 7 a)** indicates that the leakage flow in the axial clearance, interacting with the incoming main flow, is a major aeroacoustic noise source is. **Fig. 8 a)** suggests that the incoming flow, hitting the LE on the suction side due to negative incidence [conf. Fig. 8 b)] also generates significant noise.

Smaller axial clearance leads to a less intense leakage flow, and presumably less of the expected leakage flow noise. But, on the other hand, the smaller the axial clearance, the less the distance between the perforated cover and the LE, resulting in more of the expected rotor-stator interaction noise. These counteracting effects are to be considered simultaneously when judging the effect of clearance size.

4. PROTOTYPING AND TESTING

The final axial rotor geometry has iteratively been designed – and tested – with consideration of a practically relevant mean axial clearance size, allowing for a leakage flow the aerodynamic effects of which on the incidence to the LE, 3D interblade flow, and flow deviation past the TE were taken into account, by adjusting the camber line geometry. The design goal was to provide a cooling capacity represented by the datum radial fan at Φ_n. The resultant rotor, presented in Fig. 1 b), has been manufactured at the Department of Polymer Engineering, BME.

In order to judge the cooling capability of the competing fans, measurements were carried out using a Testo 875-2 thermal camera, in idle run of the electric motor, starting from the same initial state. It was found that the "hot spot" of the highest temperature is a proper quantitative indicator of the warm-up process – presented in **Figure 10** – over the entire cooling rib zone, selected as the interrogation area. Quantification of the colour scale was intentionally left non-disclosed. The figure confirms that the new axial rotor is equivalent to the datum radial one from the aspect of cooling, within the range of experimental uncertainty.

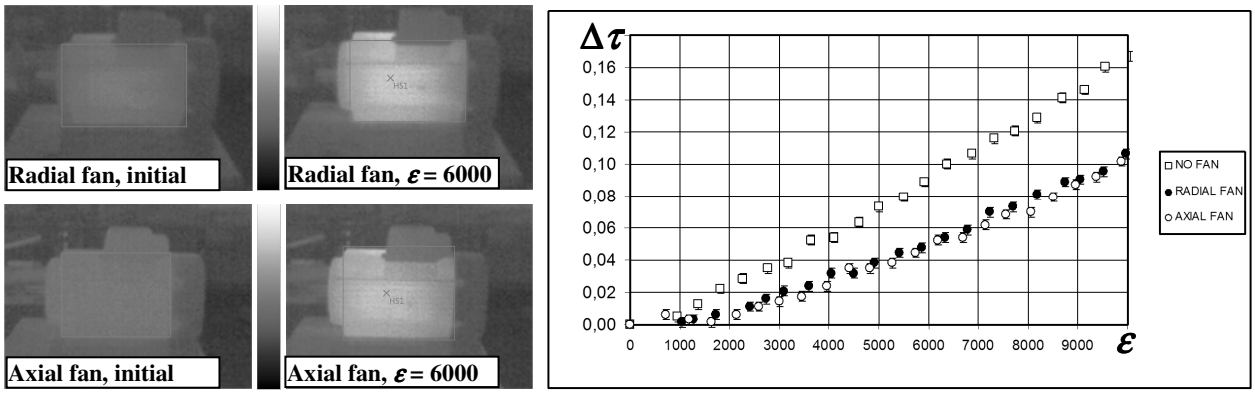

a) **b)**

Figure 10. a) Examples for thermocamera records, b) Warm-up history

It has been concluded from the test measurements that the shaft mechanical power absorbed by the axial fan is only 70 % of that of the radial fan, within the uncertainty range of ± 5 %, due to its favourable aerodynamic and energetic characteristics.

Comparative acoustic measurements were carried out in idle run. The motor has been mounted on a vibration damping board. Three measuring points were taken for each studied case. The base point was taken as fitting to the axis of rotation, on the outer surface of the fan cover. The three measuring points were taken on a horizontal plane, at a distance of 0.500 *m* from the base point: one point on the axis of rotation, and two side points in a ± 90° off-axis arrangement. The noise of the electric motor without rotor and cover was also measured, and its effect has been extracted from the

evaluation. The experimental uncertainty, dedicated mainly to repeatability error due to positioning uncertainty of the microphone, caused the variance of measurement data within a 1 d*B* range. The measurements revealed a 7.3 d*B*(A) reduction of the A-weighted SPL for the axial rotor, averaged for the three points, in comparison to the datum radial rotor.

5. SUMMARY

A CFD- and CAA-based iterative design has been carried out in order to obtain an axial fan replacing the radial fan used presently for electric motor cooling, in order to reduce fan noise and absorbed mechanical power. Testing of the datum radial and the axial rotors was carried out with the incorporation of aerodynamic, energetic, thermodynamic and acoustic experiments. The measurements revealed an approx. 30 % reduction of absorbed mechanical power and an approx. 7 d*B*(A) reduction of the A-weighted sound pressure level for the axial rotor, relative to the radial one, while the cooling capacity remained unchanged. The novel aspects of the paper are summarized as follows.

- The characteristic and efficiency curves are presented for a cooling fan with radially adjusted straight blades. η_V was found to increase nearly linearly with volume flow rate.
- The controlled vortex design method has purposefully been applied to the axial fan blades, for reducing noise, improving blade aerodynamics, and customizing the outlet axial velocity distribution to the outlet geometry – i.e. less cooling demand at lower radii; more cooling demand near the circumference, where the cooling ribs are located.
- The leakage flow developing in the axial clearance between the shroud inlet plane and the inlet plane of the cover was found to deteriorate the flow conditions along the entire span of the axial rotor blades. The blade angle at the leading edge has been re-adjusted to accommodate the flow incidence conditions influenced by the leakage flow. The flow rate delivered toward the cooling ribs was experienced to decrease nearly linearly with axial clearance size.
- The motor shield located close downstream of the axial rotor induces strong radial flow already in the blade passages, and increases the deviation of flow from the trailing edge geometry. These effects were considered in design, by modelling conical stream surfaces through the blading, and by increasing the flow turning capability of the blade sections via re-cambering and re-staggering.
- The leakage flow in the axial clearance has been recognized as a major source of axial fan noise. The following expectable trends have been outlined. Reducing the clearance presumably tends to moderate the leakage flow noise but tends to intensify the interaction noise between the rotor and the front cover. These two counteracting effects are to be simultaneously considered when judging the acoustic effect of the clearance size.

ACKNOWLEDGEMENTS

Gratitude is expressed to Grundfos Hungary Manufacturing Ltd. for initiating the presented R&D project, and for permission to publish this paper. The authors are thankful to Mr. N. Kiss, Mr. V. Paholik, and Mr. Zs. Nyeste for consultation on behalf of Grundfos. The authors express their gratitude to Dr. J. G. Kovács and Mr. G. Szebényi for manufacturing the prototype fans and for contributing to the thermocamera measurements. The paper has been supported by the Hungarian National Fund for Science and Research under contracts No. OTKA K 63704 and K 83807. The work relates to the scientific programme of the project "Development of quality-oriented and harmonized R+D+I strategy and the functional model at BME". The New Hungary Development Plan (Project ID: TÁMOP-4.2.1/B-09/1/KMR-2010-0002) supports this project.

REFERENCES

Carolus, T. (2003), *Ventilatoren*. B. G. Teubner Verlag, Wiesbaden.

Cros, S., Carbonneau, X. (2009), *Computational study of the aerodynamic impact of stall margin improvements in a high tip speed fan.* Proc. 8th European Conference on Turbomachinery Fluid Dynamics and Thermodynamics (ETC'08), Graz, Austria, pp. 401-410.

Corsini, A., Rispoli, F., Sheard, A. G. (2009), *Aerodynamic performance of blade tip end-plates designed for low-noise operation in axial flow fans.* ASME J Fluids Engineering, 131, DOI: 10.1115/1.3026723, Paper No. 081101.

Fluent 6.3.26 User's guide (2006) (Fluent Inc., Lebanon, NH, USA)

Gifford, N. L., Hunt, A. G., Savory, E., Martinuzzi, R. J. (2006), *Experimental study of low-pressure automotive cooling fan aerodynamics under blocked conditions.* CSME 2006 Forum, Kananaskis, Calgary, Canada.

Gifford, N. L., Savory, E., Martinuzzi, R. J. (2007), *Experimental study of automotive cooling fan aerodynamics.* SAE Paper No. 2007-01-1525.

Henner, M., Moreau, S., Brouckaert, J. F. (2009), *Comparison of experimental and numerical flow field in an automotive engine cooling module.* Proc. 8th European Conference on Turbomachinery Fluid Dynamics and Thermodynamics (ETC'08), Graz, Austria, pp. 387-399.

Horváth, Cs., Vad, J. (2009), *Broadband noise source model acoustical investigation on unskewed and skewed axial flow fan rotor cascades.* Proc. Conference on Modelling Fluid Flow (CMFF'09), Budapest, Hungary, pp. 682-689.

Hunt, A. G., Savory, E., Gifford, N. L., Martinuzzi, R. J. (2009), *Downstream blockage corrections of automotive cooling fan module performance.* SAE Paper No. 2009-01-0175.

ISO 3743-1:1994; ISO 3743-2:1994. *Acoustics – Determination of sound power levels of noise sources - Engineering methods for small, moveable sources in reverberant fields.*

ISO 5167-1:2003; ISO 5167-2 :2003. *Measurement of fluid flow by means of pressure differential devices inserted in circular cross-section conduits running full.*

Johnson, G., Simmons, K., Foord, C. (2007), *Experimental investigation into windage power loss from a shrouded spiral bevel gear.* ASME Paper No. GT2007-27885.

Kelecy, F., (2006), *Rotating Machinery.* In: Instructor-led training: advanced training in FLUENT. ANSYS Inc.

Lakshminarayana, B. (1996), *Fluid dynamics and heat transfer of turbomachinery.* John Wiley & Sons, Inc., New York.

Lieblein, S. (1965), *Experimental flow in two-dimensional cascades.* Chapter VI in Aerodynamic design of axial-flow compressors. Report NASA SP-36, Washington D. C.

Noda, S., Mizuno, S., Suzuki, K. (2005), *Fan noise and resonance frequency analysis in fan-cooled induction motor.* Proc. VSTech 2005, The First International Symposium on Advanced Technology of Vibration and Sound, Hiroshima, Japan, pp. 41-46.

Vad, J., Kwedikha, A. R. A., Jaberg, H. (2006), *Effects of blade sweep on the performance characteristics of axial flow turbomachinery rotors.* Proc. Instn Mech. Engrs, Part A, J. Power and Energy, 220, pp. 737-751.

Vad, J., Kwedikha, A. R. A., Horváth, Cs., Balczó, M., Lohász, M. M., Régert, T. (2007), *Aerodynamic effects of forward blade skew in axial flow rotors of controlled vortex design.* Proc. Instn Mech. Engrs, Part A, J. Power and Energy, 221, pp. 1011-1023.

Wallis, R. A. (1983), *Axial flow fans and ducts.* John Wiley & Sons, New York.